# Semipermeable lipid bilayers exhibit diastereoselectivity favoring ribose

**M. G. Sacerdote* and J. W. Szostak†**

Howard Hughes Medical Institute and Department of Molecular Biology, Massachusetts General Hospital, Boston, MA 02114

Edited by Leslie Orgel, The Salk Institute for Biological Studies, La Jolla, CA, and approved March 14, 2005 (received for review November 15, 2004)

**Nutrient uptake by a primitive cell would have been limited by the permeability characteristics of its membrane. We measured the permeabilities of model protocellular membranes to water, five of the six pentoses, and selected aldohexoses, ketohexoses, and three to six carbon alditols by following volume changes of vesicles after the addition of solute to the external medium. Solute hydrophobicities correlated poorly with permeability coefficients within one structural class of compounds. The permeability coefficients of diastereomeric sugars differed by as much as a factor of 10, with ribose being the most permeable aldopentose. Flexible alditols and sugars, sugars biased toward or restricted to furanose forms, and sugars having anomers with hydrophobic faces permeated more quickly than compounds lacking these features. Among the aldopentoses, only ribose possesses all of these properties. Ribose permeated both fatty acid and phospholipid membranes more rapidly than the other aldopentoses or hexoses. The enhanced permeability conferred by the unique conformational preferences of ribose would have allowed faster assimilation of ribose by primitive cells as they passively absorbed materials from the environment. The kinetic advantage of ribose over the other aldopentoses in crossing membranes may therefore have been one factor that facilitated the emergence of the RNA world.**

membranes | prebiotic chemistry | RNA world

RNA is thought to have acted as both the genetic and the enzymatic material during an early stage in the evolution of life, usually referred to as the RNA world (1). However, it remains unclear whether life began with an RNA genome or whether earlier forms of life used other, perhaps simpler, genetic polymers. Although compelling arguments have been made for the presence of phosphate esters in nucleic acids (2), there is as yet no similarly convincing explanation for why ribose is the sugar in the nucleic acid backbone. Oligonucleotides in which the canonical nucleobases are attached to threose (3), aldopentopyranoses, hexopyranoses, or deoxyhexopyranoses can also form stable double helices (4), some of which are more stable than RNA homoduplexes. RNA was clearly not selected for the stability of its double helices, so other factors such as preferential synthesis, stability, or reactivity must have played a role in the emergence of ribose as the sugar of life.

Ribose can be synthesized by heating aqueous formaldehyde with divalent metal ions, concentrated base, and catalytic amounts of glycolaldehdye (the "formose" reaction) (5). However, these simulated prebiotic conditions have long been known to be problematic because ribose is a very minor component of the dozens of products generated. Furthermore, the half-life of ribose under the alkaline conditions required for the condensation of formaldehyde into carbohydrates is short (6). Nevertheless, several recent findings suggest that the aldopentoses, and possibly ribose, may be favored under particular conditions. When the formose reaction is carried out at pH 9 in the presence of high concentrations of $Pb^{2+}$, the major initial products are the aldopentoses (7). The presence of calcium borate minerals, which are abundant in evaporite deposits, stabilizes ribose and the other aldopentoses by forming *cis*–diol complexes that could favor their accumulation (8). Ribose rapidly and selectively combines with cyanamide at room temperature (9) to form a sparingly soluble bicyclic derivative that readily crystallizes to yield a pure, chemically stable product (10). The ribose–cyanamide adduct reacts with cyanoacetylene to give cytidine nucleosides, but as the $\alpha$ rather than the $\beta$ anomer that occurs in biological nucleic acids (9). No mechanism has been proposed by which this process can be efficiently reversed to allow for the synthesis of $\beta$-nucleosides. Alternative chemical or physical sorting mechanisms might therefore also contribute to the prebiotic selection of ribose as the sugar of choice for nucleic acid backbones.

We hypothesized that diastereoselective membrane permeability could function as a passive sorting mechanism to enrich ribose within protocells in the prebiotic world, in a manner reminiscent of the industrial purification of various sugars by selective transport across hydrophobic membranes with synthetic complexing agents (11, 12). Vesicles composed of mixtures of fatty acids and their conjugate bases (13, 14) have been proposed as models for prebiotic membranes due to their chemical simplicity relative to phospholipid membranes, and their dynamic behaviors (15). In particular, fatty acid vesicles spontaneously assemble from micelles and lipid films, form autocatalytically (16), and grow by absorbing free fatty acids (17). Recent work in our laboratory has demonstrated that numerous minerals and clays, including montmorillonite, which is known to catalyze the nonenzymatic polymerization of activated ribonucleotides (18), also promote the formation of fatty acid vesicles, some of which encapsulate their "parent" mineral surfaces and their complements of adsorbed nucleic acids (17).

To address our hypothesis, we measured the kinetics of monosaccharide and alditol permeation across fatty acid and phospholipid membranes (19). In contrast to the modest differences in permeability coefficients between most diastereomers, ribose exhibits a substantially higher permeability coefficient relative to the other aldopentoses. Thus, membrane permeability differences provide a physical process that could have favored ribose by allowing its preferential uptake by primitive cells.

## Materials and Methods

All compounds were purchased from Sigma except for palmitoleic acid (NuChek, Elysian, MN) erythrose, threose, xylulose (Omicron Biochemicals, South Bend, IN), and the fluorophores (Molecular Probes, Eugene OR) and were used without further purification. Vesicles were prepared and diluted in 0.2 M bicine/5 mM disodium EDTA, adjusted to pH 8.5 with NaOH (subsequently referred to as 1× buffer) unless otherwise indicated. Solutions were protected from light and stored

This paper was submitted directly (Track II) to the PNAS office.

Freely available online through the PNAS open access option.

Abbreviations: POPC, 1-palmitoyl-2-oleoyl-*sn*-glycero-3-phosphocholine; DPPC, 1,2-dipalmitoyl-*sn*-glycero-3-phosphocholine; C, cholesterol; PA, 1,2-dipalmitoyl-*sn*-glycero-3-phosphate.

*Present address: Washington University School of Medicine, St. Louis, MO 63110.

†To whom correspondence should be addressed. E-mail: szostak@molbio.mgh.harvard.edu.





www.pnas.org/cgi/doi/10.1073/pnas.0408440102

under argon at room temperature. Experiments were performed at 23°C.

Fatty acid vesicles were prepared by the pH-drop method (20). Fatty acid micelles were added to buffer (1× final concentration) containing 10 mM 5-carboxyfluorescein (CF) (oleate vesicles) or 5 mM calcein (myristoleate and palmitoleate vesicles) and tumbled overnight to yield a suspension of heterogeneous vesicles (50 mM fatty acid). Crude vesicles were extruded 11 times through two 100-nm pore-size polycarbonate filters (Nucleopore, Avanti Polar Lipids, Alabaster, AL), tumbled overnight, and purified away from unencapsulated dye by size-exclusion chromatography (Sepharose 4B) using 1× buffer supplemented with 0.5 mM oleate, 2 mM palmitoleate, or 4 mM myristoleate as the eluent.

Phospholipid vesicles were prepared by dissolving 3 $\mu$mol of 1-palmitoyl-2-oleoyl-*sn*-glycero-3-phosphocholine (POPC) or 3 $\mu$mol of 1,2-dipalmitoyl-*sn*-glycero-3-phosphocholine (DPPC) mixed with cholesterol (C) and 1,2-dipalmitoyl-*sn*-glycero-3-phosphate (PA) (20:15:2 mol/mol) in 25 ml $CHCl_3$ and then depositing the lipids as thin films by rotary evaporation. Residual $CHCl_3$ was removed by lyophilization at 40 millitorr for >1 h. The film was hydrated with 1× buffer containing 10 mM 5-carboxyfluorescein (CF) and vortexed with 2-mm glass beads to yield a 10 mM solution of POPC or DPPC. POPC and DPPC/C/PA vesicles were sequentially extruded 11 times through 800-nm filters, 11 times through 400-nm filters, 11 times through 200-nm filters, and then 11 times through 100-nm filters. Unencapsulated dye was removed by size-exclusion chromatography (Sepharose 4B) using 1× buffer as the eluent.

To measure leakage, vesicles containing dye were incubated for 15–36 h with solute. They were then centrifuged for 8 min at 14,000 × *g* in Microcon YM-30 spin filters (Millipore, Bedford, MA); the starting material and filtrate were diluted into 3% Triton X-100 and the dye concentrations measured on a SpectraMAX GeminiEM fluorescence plate reader (Molecular Devices) using $\lambda_{ex}$ 470 nm, $\lambda_{em}$ 550 nm. Vesicles released <0.75% of the encapsulated dye per day. The fluorescence intensity of 5 $\mu$M calcein or 5-carboxyfluorescein (CF) decreased by ≈5% in 0.1 M solute in 1× buffer.

Vesicle sizes were ascertained by dynamic light scattering (DLS, $\lambda$ = 800 nm, 90° scattering angle) using a temperature-controlled PDDLS-Batch Analyzer (Precision Detectors, Bellingham, MA). Extruded vesicles were considered to be unilamellar, monodisperse populations in which the mean hydrodynamic diameter measured by DLS equaled the true vesicle diameter (21).

Permeability experiments were performed with either an Applied Photophysics (Surrey, U.K.) SF.17MV stopped-flow spectrofluorimeter (dead time <2 ms) or a Cary Eclipse spectrofluorimeter (Varian, Palo Alto, CA) according to the method of Chen and Verkman (22). Vesicles were mixed at a 1:1 vol/vol ratio with solute (final solute concentration, 0.1–0.5 M) in 1× buffer and fluorescence was measured at $\lambda_{ex}$ 470 nm, $\lambda_{em}$ 550 nm. Fluorescence data were converted into volumes based on a standard curve derived from experiments in which vesicles were osmotically compressed by challenge with an impermeable solute. Osmolalities were measured with a Wescor 5500 vapor pressure osmometer. Single-exponential curves were fit to the volume traces, and permeability coefficients of water ($P_f$) and solutes ($P_s$) were calculated by comparing the experimental time constants to time constants derived from one-parameter simulations (23) (see *Supporting Text*, which is published as supporting information on the PNAS web site).

Relative hydrophobicities were estimated by subjecting solutes to isocratic RP-HPLC. Solutes were passed through a 4.6 × 250 mm Alltima $C_{18}$ column (5-$\mu$m particle size, Alltech, Deerfield, IL) using water as the eluent at a flow rate of 0.75 ml/min. Solutes were detected by monitoring absorbance at 200 nm. The calculated logarithms of water–octanol partition coefficients (ClogP values) were obtained from the ClogP tool in CHEMDRAW ULTRA 7.0 (CambridgeSoft, Cambridge, MA), which uses the methodology established by the MedChem project (24).

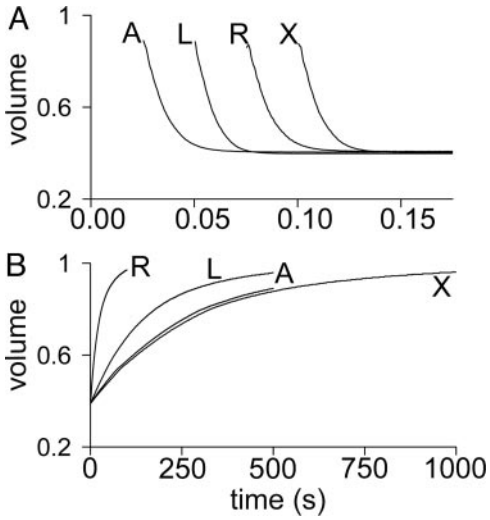


**Fig. 1.** Time courses from shrink–swell experiments with aldopentoses; *x* axis, time in seconds; *y* axis, normalized volumes. (*A*) Water efflux from large unilamellar oleate vesicles immediately after addition of 0.5 M arabinose (A), lyxose (L), ribose (R), and xylose (X). Traces translated 25 ms for clarity. (*B*) As solutes equilibrate across the oleate membrane, vesicles return to their original volumes to maintain osmotic equilibrium with the external solution. Vesicles equilibrate most rapidly in the presence of osmolytes with high permeability coefficients.

## Results

Permeability coefficients were measured by shrink–swell experiments. When challenged with hypertonic solutions of sugars or sugar alcohols, vesicles rapidly shrank because of water efflux, leading to increased self-quenching of encapsulated fluorophores. As solute concentrations equilibrated across the membrane, the vesicles expanded and fluorescence recovered to near its initial value (Fig. 1); we calculated permeabilities from the rates of the volume changes (*Supporting Text*).

Solute permeability coefficient ($P_s$, Table 1) trends were consistent when membranes of different compositions were compared (Fig. 2). On average, increasing alditol chain length from four carbons to five carbons reduced $P_s$ by ≈10-fold, and adding a sixth carbon reduced $P_s$ an additional 35-fold. Among the sugars, the aldopentoses were 50-fold more permeable than the aldohexoses. The data were highly reproducible (range, ±3.5%; $n \geq 3$) within a given batch of vesicles, with typical batch-to-batch deviations of ≈20%.

Sugar and alditol isomers sometimes exhibited significantly different permeabilities. Ribose was 6–10 times more permeable than xylose, the least permeable of the aldopentoses. $P_s$ for fructose and sorbose were roughly equal but 30 times larger than the $P_s$ of glucose, a constitutional isomer. Although permeability differences among the acyclic hexitols tested did not exceed 4- to 5-fold, inositol crossed palmitoleate membranes so slowly that we were unable to measure its permeability coefficient ($P_s < 10^{-11}$ cm/s). Both enantiomers of xylose exhibited $P_f$ and $P_s$ values that were identical within experimental error in all membranes tested, including those with chiral headgroups (POPC and DPPC/C/PA membranes).

We next examined the relationship between hydrophobicity and permeability. Water–organic partitioning was examined by using RP-HPLC. Based on elution times, longer alditols and

BIOPHYSICS

**Table 1. Solute permeability coefficients ($P_s$) across fatty acid and phospholipid membranes**

| | Membrane composition | | | | | |
|---|---|---|---|---|---|---|
| Solute | Myristoleate* | Palmitoleate* | Oleate* | Oleate† | POPC* | DPPC/C/PA‡ |
| Glycerol§ | | | 490 | | | |
| Erythritol§ | 28 | 14 | 12 | 4.8 | 21 | |
| DL-Threitol | 50 | 23 | 22 | 11 | 40 | |
| Adonitol | 2.9 | 1.7 | 0.91 | 0.38 | | |
| Arabitol | 2.1 | 1.4 | 0.63 | 0.39 | | |
| Xylitol | 5.0 | 3.0 | 1.8 | 0.95 | | |
| Dulcitol | | | | 0.013 | | |
| Mannitol | 0.051 | 0.015 | 0.0058 | 0.0058 | | |
| Sorbitol | 0.18 | 0.071 | 0.026 | 0.027 | | |
| Arabinose | 3.5 | 2.1 | 1.1 | 0.49 | 2.8 | 1.1 |
| Lyxose | 5.7 | 3.2 | 1.9 | 0.84 | 4.5 | 1.2 |
| Ribose | 31 | 15 | 11 | 2.9 | 20 | 9 |
| D-Xylose | 3.4 | 1.9 | 0.98 | 0.51 | 2.8 | 1.0 |
| L-Xylose | 3.3 | 1.9 | 0.94 | | 2.7 | |
| Ribulose | | | 31 | | | |
| Galactose | 0.060 | 0.024 | 0.011 | 0.0086 | | |
| Glucose§ | 0.047 | 0.017 | 0.0071 | 0.0050 | | |
| Mannose | 0.10 | 0.035 | 0.018 | 0.014 | | |
| Fructose§ | 1.1 | 0.68 | | | | |
| L-Sorbose | 0.88 | 0.56 | | | | |

Values reported in $10^{-8}$ cm/s. Chiral solutes are D-enantiomers unless otherwise noted.
*Experiments performed at 23°C in 1 buffer, 0.5 M solute.
†Conditions as above but with 0.1 M solute.
‡Conditions as above, values are relative initial slopes only (D-xylose set to 1.0).
§Literature $P_s$ values across lecithin membranes: glycerol, $540 \times 10^{-8}$ cm/s (33); erythritol, $75 \times 10^{-8}$ cm/s (34); glucose, $0.003 \times 10^{-8}$ cm/s (35); and fructose, $0.04 \times 10^{-8}$ cm/s (35).

sugars appeared more hydrophilic than their shorter congeners, and stereochemistry had little influence on retention times (Table 2, which is published as supporting information on the PNAS web site). The hydrophobicity of each compound was also calculated as the average ClogP of its acyclic, furanose, and pyranose forms weighted for the amounts present at equilibrium. The high proportion of furanose forms of ribose in solution slightly elevated the overall ClogP of ribose relative to the other aldopentoses; nevertheless, ribose and mannitol emerge as outliers when $\log(P_s)$ is plotted against ClogP (Fig. 3).

To determine whether solutes were perturbing the membranes, water permeability coefficients ($P_f$) were measured as a function of solute identity, membrane composition, and solute concentration (Table 3, which is published as supporting information on the PNAS web site). $P_f$ did not vary when vesicles were challenged with different solutes at equal concentrations. At a solute concentration of 0.5 M, myristoleate, palmitoleate, oleate, POPC, and DPPC/C/PA membranes had average $P_f$ values of $17 \times 10^{-3}$, $10 \times 10^{-3}$, $8.4 \times 10^{-3}$, $7.0 \times 10^{-3}$, and $0.27 \times 10^{-3}$ cm/s, respectively. Oleate membrane permeability to water increased with solute concentration in a solute-independent manner (Fig. 4, which is published as supporting information on the PNAS web site). Extrapolating to zero solute concentration yielded an oleate $P_f$ of $6.4 \times 10^{-3}$ cm/s.

## Discussion

Ribose is surprisingly more membrane permeable than the other aldopentose sugars, which diffuse across membranes 3- to 10-fold more slowly. In general, sugar and alditol permeabilities across lipid bilayers follow the predictions of Overton's rule: increasing hydrophilicity decreases the solute permeability $P_s$. Increasing sugar or alditol chain length and hence decreasing solubility in the hydrophobic interior of a bilayer membrane decreases permeability, as expected. However, the predictive value of Overton's rule decreases when classes of related compounds with similar hydrophobicities are considered. Isomeric sugars and alditols exhibit only a weak correlation between measured or calculated hydrophobicity and permeability. Thus, additional second-order properties of the solute must be considered. The consistency of the permeability trends in five different membrane systems (Fig. 3) led us to believe that the differences are due to intrinsic qualities of the solutes rather than specific solute–membrane interactions. We investigated several possible explanations for these second-order effects on permeability.

We first explored the hypothesis that the various solutes were selectively permeabilizing the membranes. Had the solutes differentially intercalated into the membrane or coated the vesicles, one would expect the nature of the solute to influence the water permeability. Some membrane perturbation occurs, as shown by a positive correlation between solute concentration and permeability to water, but this effect was invariant from solute to solute (Table 3 and Fig. 4). None of the solutes induced vesicles to leak encapsulated fluorophores. Carbohydrate interactions with membrane headgroups are known to occur, as shown by previous work with phospholipid membranes indicating that sucrose can displace the shell of ordered water at the headgroup-solvent interface (25). A similar displacement might be related to the solute-specific concentration dependence of permeability coefficients for the aldopentoses. However, both xylose enantiomers permeated membranes at equal rates, regardless of whether headgroups were chiral or achiral, suggesting that solute-headgroup interactions are probably not rate-determining.

Two factors which may influence solute permeabilities are conformation and flexibility. Molecular dynamics simulations (26), proton NMR (27), and crystal structures (28) show that some alditols prefer kinked conformations to straight-chain structures to avoid *syn*–pentane interactions between hydroxyl groups. Interconversion between rotamers is rapid at room temperature, but the greater rotational freedom in solution of

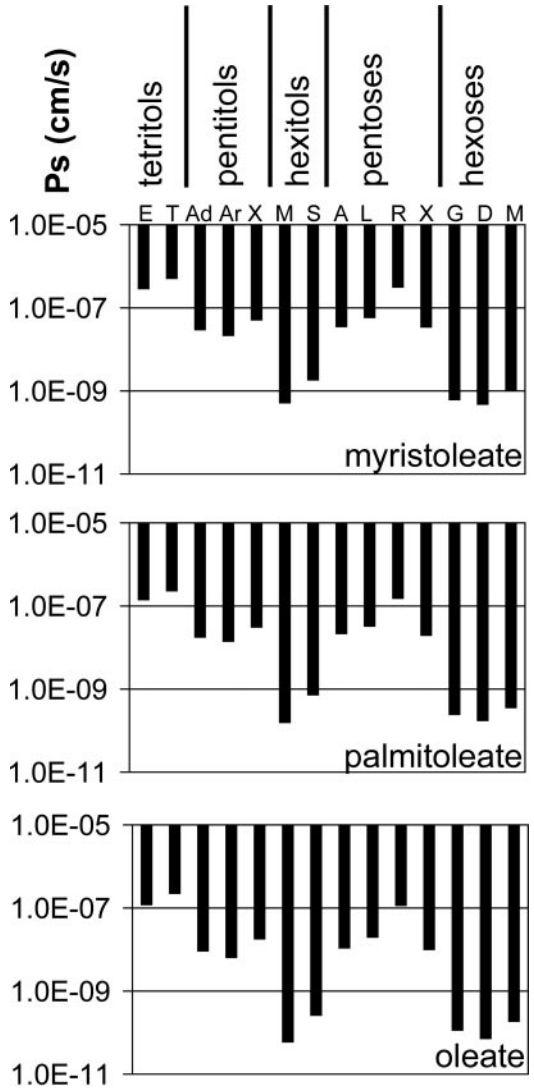


**Fig. 2.** Relative permeability coefficients were nearly identical in all membranes tested. Tetritols: erythritol (E) and threitol (T). Pentitols: adonitol (Ad), arabitol (Ar), and xylitol (X). Hexitols: mannitol (M) and sorbitol (S). Pentoses: arabinose (A), lyxose (L), ribose (R), and xylose (X). Hexoses: galactose (G), glucose/dextrose (D), and mannose (M). See Table 1 for exact values. Note the log scale.

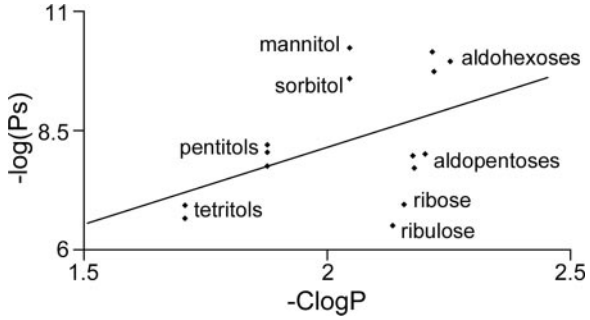


**Fig. 3.** Relation between calculated water–octanol partition coefficient (ClogP) and permeability coefficient ($P_s$). Mannitol, ribose, and ribulose deviate highly from the trend line.

xylitol compared to adonitol (ribitol) and arabitol correlates with a higher permeability coefficient (27). Likewise, sorbitol (glucitol) is more flexible than dulcitol (galactitol) and mannitol (29, 30) and permeates most quickly among the hexitols tested, whereas inositol, conformationally locked by its cyclic structure, exhibits a drastically lowered permeability ($P_s < 10^{-11}$ cm/s, palmitoleate membranes). Molecular dynamics simulations indicate that greater rotational freedom reflects interaction with fewer solvent molecules (26). The acyclic alditols often permeated as rapidly as their corresponding sugars, which is surprising because cyclization of a sugar results in the net replacement of a carbonyl (or its hydrated *gem*–diol form) with an ether. A possible explanation for the similarity in permeability coefficients between alditols and aldoses is that the increase in hydrophobicity due to cyclization is offset by the loss of conformational freedom associated with ring closure.

Combining our observations regarding the acyclic alditols with conformational analysis provided some clues as to why ribose is unusually permeable. First, equilibrium solutions of ribose contain a large proportion of furanose forms (≈20%). This property should enhance the permeability of ribose because, according to logP calculations, furanoses are inherently more hydrophobic than pyranoses. Consistent with this hypothesis, fructose and ribulose had relatively high permeabilities, whereas glucose and xylose had relatively low permeabilities. Qualitatively, other sugars restricted to furanose rings such as xylulose, erythrose, and threose exhibited high permeabilities, but the data for these three sugars were too noisy to quantitate. Second, because ring-opening constants are ≈20-fold higher for furanoses than for pyranoses (31), a consequence of the furanose bias of ribose is increased flexibility (31). This finding agrees with the data indicating that rotationally less restricted alditols permeate faster than rigid alditols. Third, the α-pyranose anomer of ribose possesses a hydrophobic face without hydroxyls; moreover, many of the H-bond donors and acceptors from the hydroxyls on the hydrophilic face are internally satisfied. Observations that erythrose permeates faster than threose and that ribulose permeates faster than xylulose add weight to the possible importance of a hydrophobic face. Indeed, ribulose exhibits the highest permeability/hydrophobicity ratio of any of the pentoses or hexoses examined, although as a keto-sugar it is not expected to be easily converted into nucleotides, making a ribulose nucleic acid unlikely. Interestingly, some bile salts in which all of the hydroxyls protrude from the same face are thought to aggregate in organic solvents by forming intermolecular hydrogen bonds, thereby exposing only the hydrophobic faces of the cholesterol backbones to solvent (32). Thus, ribose may permeate as α-pyranose dimers, a conjecture supported by the higher concentration dependence of the permeability coefficient of ribose relative to those of the other aldopentoses (Table 1, compare columns 3 and 4). Permeability studies of the conformationally locked aldopentose methyl glycosides might permit rigorous testing of this hypothesis.

The diastereoselectivity of semipermeable fatty acid and phospholipid membranes for ribose means that primitive cells might have had better access to ribose than the other aldopentoses. This is a purely kinetic effect, in that no difference in equilibrium concentrations is expected. However, if metabolic processes within the cell converted externally supplied sugars into products such as nucleotides and/or polynucleotides, those transformations could have been limited by the spontaneous permeation of the sugar across the membrane barrier. Rate-limiting nutrient uptake apparently occurred frequently during the history of life, hence the evolution of the numerous sugar, amino acid, and ion transporters that now constitute a large fraction of many bacterial genomes. Before the evolution of protein transporters, differences in the un-

catalyzed rates of membrane permeation may at times have been very significant, and cells dependent on ribose could have had a selective advantage over cells dependent on the more slowly permeating aldopentoses arabinose, lyxose, and xylose. Four-carbon sugars such as threose do enter even more rapidly than ribose, and if abundant, might have led to an advantage for a polymer such as threose nucleic acid. However, if prebiotic chemical processes supplied a mixture of the four aldopentoses, the greater membrane permeability of ribose might have been one factor (among others such as differential synthesis, decay, conversion to nucleotides, and properties of the resulting nucleic acids) that favored its emergence as the sugar of life.

We thank Keith Miller for use of his stopped-flow spectrofluorimeter, Alfred Van Hoek and Enrique Arevalo for advice and technical assistance, and Steven A. Benner for helpful discussions. J.W.S. is an Investigator of the Howard Hughes Medical Institute. This work was supported in part by National Aeronautics and Space Administration Exobiology Program Grant EXB02-0031-0018.

1. Gilbert, W. (1986) *Nature* **319,** 618.
2. Westheimer, F. H. (1987) *Science* **235,** 1173–1178.
3. Schoning, K.-U., Scholz, P., Wu, X., Guntha, S., Delgado, G., Krishnamurthy, R. & Eschenmoser, A. (2002) *Helv. Chim. Acta* **85,** 4111–4153.
4. Beier, M., Reck, F., Wagner, T., Krishnamurthy, R. & Eschenmoser, A. (1999) *Science* **283,** 699–703.
5. Breslow, R. (1959) *Tetrahedron Lett.* **21,** 22–26.
6. Larralde, R., Robertson, M. P. & Miller, S. L. (1995) *Proc. Natl. Acad. Sci. USA* **92,** 8158–8160.
7. Zubay, G. (1998) *Origins Life Evol. Biosph.* **28,** 13–26.
8. Ricardo, A., Carrigan, M. A., Olcott, A. N. & Benner, S. A. (2004) *Science* **303,** 196.
9. Sanchez, R. & Orgel, L. E. (1970) *J. Mol. Biol.* **47,** 531–543.
10. Springsteen, G. & Joyce, G. F. (2004) *J. Am. Chem. Soc.* **126,** 9578–9583.
11. Tbeur, N., Rhlalou, T., Hlaibi, M., Langevin, D., Metayer, M. & Verchere, J. F. (2000) *Carbohydr. Res.* **329,** 409–422.
12. Duggan, P. J. & Szydzik, M. L. (2003) *Aust. J. Chem.* **56,** 17–21.
13. Gebicki, J. M. & Hicks, M. (1973) *Nature* **243,** 232–234.
14. Gebicki, J. M. & Hicks, M. (1976) *Chem. Phys. Lipids* **16,** 142–160.
15. Chen, I. A. & Szostak, J. W. (2004) *Proc. Natl. Acad. Sci. USA* **101,** 7965–7970.
16. Oberholzer, T., Wick, R., Luisi, P. L. & Biebricher, C. K. (1995) *Biochem. Biophys. Res. Commun.* **207,** 250–257.
17. Hanczyc, M. M., Fujikawa, S. M. & Szostak, J. W. (2003) *Science* **302,** 618–622.
18. Ertem, G. & Ferris, J. P. (1996) *Nature* **379,** 238–240.
19. Bittman, R. & Blau, L. (1986) *Biochim. Biophys. Acta* **863,** 115–120.
20. Monnard, P. A. & Deamer, D. W. (2003) *Methods Enzymol.* **372B**, 133–151.
21. MacDonald, R. C., MacDonald, R. I., Menco, B. P., Takeshita, K., Subbarao, N. K. & Hu, L. (1991) *Biochim. Biophys. Acta* **1061,** 297–303.
22. Chen, P. Y. & Verkman, A. S. (1988) *Biochemistry* **27,** 5713–5718.
23. Mazur, P., Leibo, S. P. & Miller, R. H. (1974) *J. Membr. Biol.* **15,** 107–136.
24. Leo, A. J. (1993) *Chem. Rev.* **93,** 1281–1306.
25. Disalvo, E. A. (1988) *Adv. Colloid Interface Sci.* **29,** 141–170.
26. Grigera, J. R. (1988) *J. Chem. Soc. Faraday Trans. 1* **84,** 2603–2608.
27. Franks, F., Kay, R. L. & Dadok, J. (1988) *J. Chem. Soc. Faraday Trans. 1* **84,** 2595–2602.
28. Jeffrey, G. A. & Kim, H. S. (1970) *Carbohydr. Res.* **14,** 207–216.
29. Ranganathan, M. & Rao, V. S. R. (1981) *Curr. Sci.* **50,** 933–936.
30. Angyal, S. J. (1980) *Carbohydr. Res.* **84,** 201–209.
31. Wertz, P. W., Garver, J. C. & Anderson, L. (1981) *J. Am. Chem. Soc.* **103,** 3916–3922.
32. Lindenbaum, S. & Vadnere, M. (1984) in *Reverse Micelles*, eds. Luisi, P. L. & Straub, B. E. (Plenum, New York), pp. 239–259.
33. Orbach, E. & Finkelstein, A. (1980) *J. Gen. Physiol.* **75,** 427–436.
34. Vreeman, H. J. (1966) *Proc. Koninkl. Ned. Acad. Wet. Ser. B* **69,** 542–577.
35. Brunner, J., Graham, D. E., Hauser, H. & Semenza, G. (1980) *J. Membr. Biol.* **57,** 133–141.